Total-scattering cross-section measurements for intermediate-energy positrons and electrons colliding with Kr and Xe

M. S. Dababneh,* Y.-F. Hsieh, W. E. Kauppila, V. Pol,† and T. S. Stein
Department of Physics and Astronomy, Wayne State University, Detroit, Michigan 48202
(Received 8 February 1982)

Total-scattering cross sections have been measured in the same apparatus for positrons and electrons colliding with krypton and xenon in the energy range from 20 to 800 eV with the use of a beam-transmission technique. The unusual shapes of the peaks in the e^+-Kr and e^+-Xe total-cross-section curves suggest the possibility that inelastic processes may be contributing significantly to the respective total cross sections in those peaks. A distinct shoulder exists in the e^--Xe total-cross-section curve in the vicinity of 20 eV, followed by a rapid decrease with the electron results dropping below the corresponding positron results in the energy range from 40 to 90 eV. This crossing of the curves at these energies is somewhat anomalous compared to the situation for the other inert gases, where the electron results remain higher than the positron results. Estimates are made of potential experimental errors, including that associated with incomplete discrimination against small-angle forward scattering.

I. INTRODUCTION

Comparisons between positron- and electron-atom scattering reveal some interesting differences and similarities. The static interaction is attractive for electrons and repulsive for positrons, while the polarization interaction is attractive for both projectiles. The exchange interaction contributes to electron scattering but does not play a role in positron scattering. Two phenomena that can occur only for positron scattering are free annihilation, appreciable only for energies much less than 1 eV, and positronium formation, which has been found to be an important factor in positron-gas scattering experiments. The combined effect of the static and polarization interactions is that they add to each other in electron scattering, whereas there is a tendency toward cancellation in positron scattering resulting in smaller total cross sections, in general, for positrons than for electrons at low energies. As the projectile energy is increased, the polarization and exchange interactions eventually become negligible compared with the static interaction (which has the same magnitude for positrons and electrons). This results in a merging of the corresponding positron and electron scattering cross sections at sufficiently high projectile energies, with their values being given by the first-Born approximation. Recent measurements by Kauppila *et al.*[1] revealed a merging of the total-scattering cross sections for positrons and electrons colliding with helium at a much lower energy (200 eV) than was predicted (2000 eV) by a distorted-wave second-Born approximation calculation of Dewangen and Walters.[2] The measurements of Kauppila *et al.*[1] did not indicate any merging of the $e^{\pm}$-Ne or $e^{\pm}$-Ar total cross sections up to the highest energies studied (700 and 800 eV, respectively). The present measurements extend our intermediate-energy total-cross-section (Q_T) investigations to Kr and Xe. As was the case for our earlier inert-gas Q_T measurements,[1,3–6] the same apparatus and experimental technique is used for the positron and electron measurements. As a result, the comparisons between the present electron and positron measurements should have added significance, since several of the potential sources of experimental errors will affect the measurements for each projectile in the same way.

II. EXPERIMENTAL APPROACH AND ERROR ANALYSIS

The experimental apparatus and procedure used in the present total-scattering cross-section measurements have been discussed in detail elsewhere,[1,3–5] and only a brief overview will be presented here. A Van de Graaff accelerator is used to generate a ^{11}C positron source by the reaction $^{11}B(p,n)^{11}C$. A variable-energy positron beam [energy width <0.1 eV (Ref. 7)] is extracted from the ^{11}C source and guided by a weak, axial magnetic field through a curved, differentially pumped gas scattering region to the detector (a Channeltron

electron multiplier). For electron measurements, the positron source is replaced by a thermionic electron source (type-B Philips cathode).

Total-scattering cross sections (Q_T) are determined by measuring the attenuation of the projectile beam as it passes through the gas scattering region and by using the expression,

$$I = I_0 e^{-nLQ_T}, \tag{1}$$

where I_0 is the detected beam intensity with no gas in the scattering region, I is the detected beam intensity with gas of number density n in the scattering region, and L is the path length of the projectile beam through the scattering region. Any errors in the determination of the measurable quantities in Eq. (1) will result in errors in the values of Q_T obtained from that equation. The error estimates listed in Table I were obtained using the same procedure as outlined by Kauppila *et al.*[1] The reported "experimental error" estimates are obtained by taking the square root of the sum of the squares of each individual error component contributing to the potential errors in I, I_0, n, and L, as well as the statistical error. The "maximum errors" are obtained from the direct addition of each individual error component. The total errors for the positron and electron comparison cross-section measurements are smaller than those for the absolute total-cross-section measurements for the same target gas, because several of the individual error components would affect both the positron and electron measurements equally. A standard check made in every data run is to measure cross sections for several different target-gas densities to ensure that the results are independent of n. Figure 1 shows the results of such tests for several different projectile, energy, and gas combinations.

Another source of error, not included in Table I, is due to incomplete discrimination against projectiles scattered at small angles in the forward direction. Two independent aspects of the present experiment that provide discrimination against small-angle scattering are (1) the use of a retarding potential field after the scattering region, which acts as a potential barrier for inelastically scattered projectiles and for projectiles elastically scattered at sufficiently large forward angles, and (2) the use of a small exit aperture (diameter = 4.76 mm) from the scattering region. An analysis of these effects by Kauppila *et al.*[1] [refer to Eqs. (6) and (10) of Ref. 1] has been used to obtain the discrimination angles (listed in Table II) for the present experiment provided by the retarding potential procedure and by the small exit aperture, respectively. Since the estimates of these discrimination angles are independent of each other, the smaller angle for each projectile, energy, and target combination should represent an upper-limit estimate of the angular discrimination. In making total-cross-section measurements we attempt to optimize the tuning of our beam-controlling parameters (lens elements and magnetic fields) for the lowest feasible magnetic

TABLE I. Estimated percentage errors in the present absolute and $e^{\pm}$ comparison total-cross-section measurements. The "experimental errors" are shown outside the parentheses while the "maximum errors" are enclosed by the parentheses. The statistical errors in this table are typical values with the actual values for each data point listed in the Appendix. The estimated errors in this table do not include the potential errors associated with discrimination against small-angle scattering, which are discussed separately.

	Projectile	
	e^+	e^-
Statistical	2(2)	1(1)
I, I_0	3(4)	2(2.5)
n	4(7)	4(7)
L	2(3)	1(2)
Total (absolute)	6(16)	5(12.5)
Total ($e^{\pm}$ comparison)	4(8)	3(4.5)

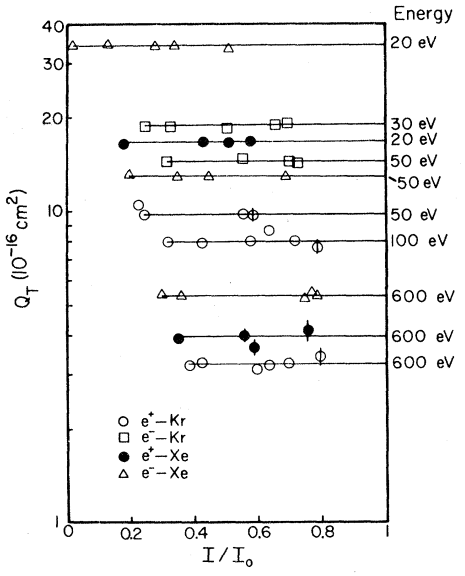

FIG. 1. Measured total cross sections vs attenuation ratio I/I_0 for various projectile-target combinations. Statistical uncertainties of one standard deviation are represented by the bars except where they are encompassed by the symbols.

TABLE II. Estimated angular discrimination (in degrees) for the retarding potential procedure (R values) and for the effect due to the exit aperture size (A values). The columns are also labeled according to the target gases and projectile particles.

	Krypton		Xenon	
	e^+	e^-	e^+	e^-
E (eV)	R,A	R,A	R,A	R,A
20	17,24	7,5	21,12	6,5
50	18,20	6,5	17,11	5,5
100	18,17	4,5	15,11	4,5
200	16,8	3,5	10,10	6,5
500	19,9	5,5	9,10	5,5
750	15,8	5,5	22,8	5,5

fields in the scattering region in order to obtain the best possible angular discriminations. The estimated angular discriminations listed in Table II for the electron total-cross-section measurements are smaller (and show less variation with energy) than those for the positron measurements, because it is much easier to optimize the beam-controlling parameters for the more intense (typically ten times larger) electron-beam currents that are used. The larger variations for positrons could result in correspondingly larger variations in the measured positron total-cross-section values.

In order to use the angular-discrimination information listed in Table II to determine the amounts by which the measured total cross sections are too low, detailed information is required on the differential elastic scattering cross sections and (depending on the projectile energies) inelastic scattering cross sections. Since the retarding potential in the present experiment is generally set within a few tenths of a volt of the projectile energy for energies less than 100 eV, and within a few volts for energies up to 800 eV, there should be very nearly 100% discrimination against inelastic scattering for Kr and Xe where the minimum energy lost by inelastically scattered projectiles is more than 5 eV.

III. RESULTS AND DISCUSSION

In the following discussions of the present total-cross-section measurements, it should be realized that the estimated angular discriminations given in Table II could affect both the reported absolute total-cross-section values and the comparisons between the positron and electron measurements on the same target gas. The present total-cross-section measurements and the associated statistical uncertainties are listed in the Appendix.

A. $e^{\pm}$-Kr

The present total-cross-section results for intermediate-energy positrons colliding with krypton are shown in Fig. 2 along with the prior experimental results of Canter *et al.*[8] and Coleman *et al.*,[9] both of which are considerably lower than the present results for energies above 20 eV. This situation is consistent with that for e^+-He, Ne, and Ar collisions where the intermediate-energy total-cross-section measurements of Canter *et al.*[8] and Coleman *et al.*[9] are generally lower than those of Jaduszliwer *et al.*,[10] Tsai *et al.*,[11] Brenton *et al.*,[12,13] Griffith *et al.*,[14] and Kauppila *et al.*[1] As discussed by Coleman *et al.*[9] and Griffith *et al.*,[14] respectively, the intermediate-energy measurements of Canter *et al.*[8] and Coleman *et al.*[9] were too low due to incomplete discrimination against small-angle scattering. Although the present e^+-Kr results are significantly higher than the prior measurements, our results may still be low

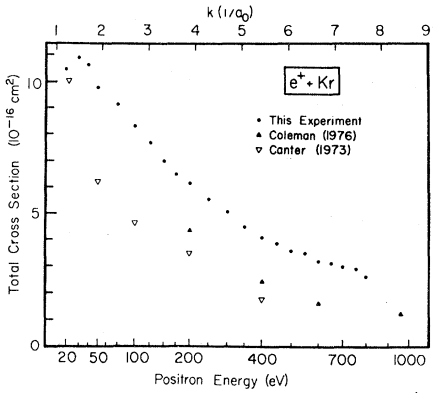

FIG. 2. Total e^+-Kr scattering cross sections. The present results are shown with the experimental data of Canter *et al.* (Ref. 8) and Coleman *et al.* (Ref. 9). The statistical uncertainties for the present results are listed in the Appendix.

due to small-angle elastic scattering. Using phase shifts (up to $l=6$) calculated by McEachran *et al.*,[15] and higher-order phase shifts (up to $l=20$) given by the Born term in the effective range expansion of O'Malley *et al.*,[16] along with the angular-discrimination data listed in Table II and an estimate of the ratio (0.55 at 20 eV) of the elastic to the total-scattering cross section (based on an extrapolation of the low-energy Q_T measurements of Dababneh *et al.*[6] from below the positronium formation threshold), we estimate that our e^+-Kr results near 20 eV could be about 10% too low due to incomplete discrimination against small-angle scattering.

The present results for intermediate-energy electrons colliding with krypton are shown in Fig. 3 along with prior experimental[17–19] and theoretical results.[20] The present e^--Kr results average 7% lower and agree in shape with those of Wagenaar and de Heer.[19] The semiempirical results of de Heer *et al.*[18] average 6% lower below 75 eV and are in good agreement (within 3%) with our results above 75 eV. The measurements of Ramsauer[17] average 30% lower than ours. The optical model (OM) theoretical results shown in Fig. 3, which average about 25% lower than the present results, were obtained from the differential elastic cross sections and total inelastic cross sections of McCarthy *et al.*[20] Using the differential and inelastic cross-section results of McCarthy *et al.*[20] and our angular-discrimination values listed in Table II, we estimate that our e^--Kr total cross sections could be 2%, 4%, 13%, and 15% low at 20, 100, 500, and 750 eV, respectively, due to incomplete discrimination against small-angle scattering. If our results were adjusted for the above percent-error estimates they would average about 5% lower below 100 eV, be in good agreement (within 2%) between 100 and 250 eV, and would average about 7% higher than the measurements of Wagenaar and de Heer[19] above 250 eV. Wagenaar and de Heer[19] have estimated their angular discrimination to be less than 1°, which would result in an error in their total-cross-section measurements (due to small-angle scattering) of less than 1%. These estimated corrections for small-angle scattering using the theoretical results of McCarthy *et al.*,[20] would slightly improve the absolute value comparisons but disrupt the good agreement that exists between the relative shapes of the present experimental results and those of Wagenaar and de Heer.[19]

A comparison of the present $e^{\pm}$-Kr total-cross-section measurements in Fig. 4 suggests that the peak in the electron curve appears to be associated with elastic scattering, since it occurs just above the lowest inelastic threshold, whereas the peak in the positron curve appears (from the shape of the curve) to be associated with inelastic scattering. In addition to the rapid increase of the e^+-Kr total cross

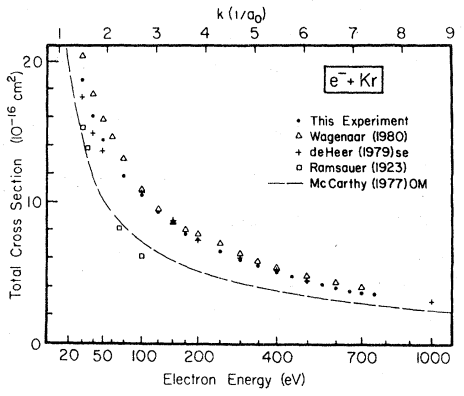

FIG. 3. Total e^--Kr scattering cross sections. The present results are shown with the experimental data of Ramsauer (Ref. 17), Wagenaar and de Heer (Ref. 19), the semiempirical (se) results of de Heer *et al.* (Ref. 18), and the optical model (OM) theoretical results of McCarthy *et al.* (Ref. 20).

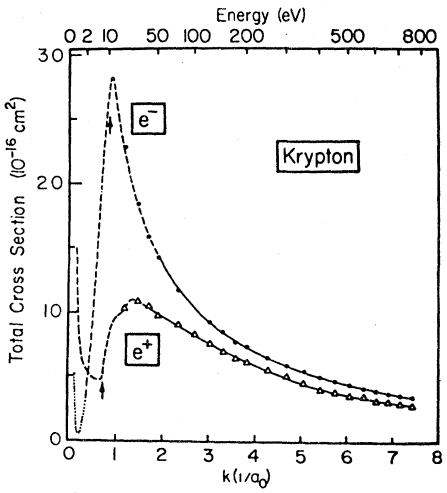

FIG. 4. A comparison of the total $e^{\pm}$-Kr cross-section measurements. The present intermediate-energy measurements are indicated by the symbols. The solid curves are drawn through the present intermediate-energy results above the range of the earlier low-energy measurements of Dababneh *et al.* (Ref. 6), which are represented by dashed curves. The low-energy electron measurements of Ramsauer (Ref. 17) are represented by the dotted curve. The lowest-energy inelastic thresholds for each projectile are indicated by arrows and correspond to positronium formation at 7.20 eV for positrons and atomic excitation at 9.91 eV for electrons.

section at the threshold for positronium formation, there appears to be a small bump (possibly associated with another inelastic process) located a few eV above the ionization threshold (14.00 eV) of Kr. From 100 to 750 eV (the highest energy studied) the electron results remain approximately 20% higher than the corresponding positron results.

B. $e^{\pm}$-Xe

The present intermediate-energy e^+-Xe total-cross-section results are shown in Fig. 5 along with prior experimental results.[21,22] The present results are much higher than the measurements of Canter *et al.*[21] and are 15-35 % higher than those of Coleman *et al.*[22] at the energies of overlap. Using phase shifts (up to $l=6$) calculated by McEachran *et al.*[15] and higher-order phase shifts (up to $l=20$) given by the Born term in the effective-range expansion of O'Malley *et al.*,[16] along with the angular-discrimination data listed in Table II, and an estimate of the ratio (0.57 at 20 eV) of the elastic to the total-scattering cross section (based on an extrapolation of the low-energy Q_T measurements of Dababneh *et al.*[6] from below the positronium formation threshold), we estimate that our e^+-Xe total-cross-section results near 20 eV could be about 10% too low due to small-angle scattering.

The present intermediate-energy e^--Xe total-cross-section results are shown in Fig. 6 along with prior experimental[18,19] and theoretical[20] results. The semiempirical results of de Heer *et al.*[18] are in excellent agreement (averaging about 1% higher) with the present results from 100 to 700 eV, but

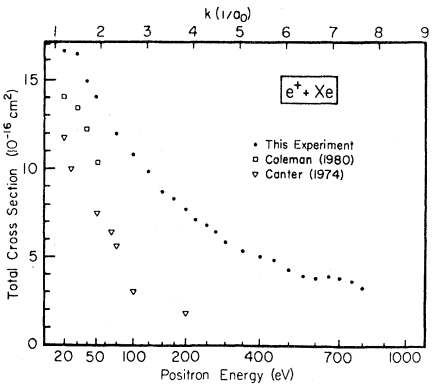

FIG. 5. Total e^+-Xe scattering cross sections. The present measurements are shown with the experimental data of Canter *et al.* (Ref. 21) and Coleman *et al.* (Ref. 22).

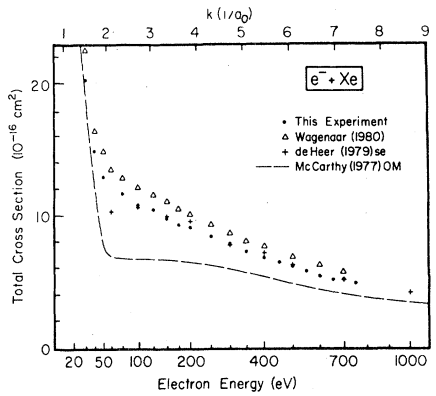

FIG. 6. Total e^--Xe scattering cross sections. The present results are shown with the experimental data of Wagenaar and de Heer (Ref. 19), the semiempirical (se) results of de Heer *et al.* (Ref. 18), and the optical model (OM) theoretical results of McCarthy *et al.* (Ref. 20).

differ significantly below 100 eV, ranging from 17% lower (at 60 eV where our value is interpolated) to 58% higher (at 30 eV) than the present results. (The values of de Heer *et al.*[18] at 20 and 30 eV are 30.9×10^{-16} and 32.0×10^{-16} cm^2, respectively, and thus are not shown in Fig. 6.) Our results average 11% lower than the experimental results of Wagenaar and de Heer[19] and agree very well in shape. The optical model (OM) theoretical results shown in Fig. 6, obtained from the differential elastic cross sections and total inelastic cross sections of McCarthy *et al.*,[20] suggest a roughly similar shape, but exhibit a more pronounced decrease than the experimental results from 20 to 60 eV, and are about 45% below the present measurements in the vicinity of 60 eV. Using the differential and inelastic cross-section results of McCarthy *et al.*[20] and our angular-discrimination values listed in Table II, we estimate that our e^--Xe total cross sections could be 4%, 8%, 16%, and 18% low at 20, 100, 500, and 750 eV, respectively, due to incomplete discrimination against small-angle scattering. If our results were adjusted for the above percent-error estimates, they would average about 7% lower below 100 eV, be in reasonable agreement (within 4%) between 100 and 200 eV, and average about 6% higher above 250 eV than the measurements of Wagenaar and de Heer[19] (whose estimated angular discrimination of less than 1° would result in an error in their total-cross-section measurements of less than 1%). As was the case for krypton, these estimated corrections for small-angle scattering, using the theoretical results of McCarthy *et al.*,[20] would slightly improve the absolute value comparisons but disrupt the good agreement that

exists in the relative shapes of the present experimental results and those of Wagenaar and de Heer.[19] However, one should be cautious in interpreting the percent-error estimates based on the calculations of McCarthy *et al.*,[20] since their calculations yield total-cross-section results for e^--Kr and Xe scattering, whose detailed shapes and magnitudes differ noticeably from the experimental results shown in Figs. 3 and 6, respectively.

A comparison of the present intermediate-energy $e^{\pm}$-Xe measurements in Fig. 7 reveals some interesting features in the nature of these respective curves. A distinctive feature in the e^--Xe curve is the shoulder near 20 eV, which is followed by a rapid decrease in the measured total cross section between 20 and 50 eV, with the electron curve dropping below the positron curve from 40 to 90 eV. Such a crossing of the e^+ and e^- cross sections at energies above 20 eV has not been observed for any of the other inert gases (refer to the $e^{\pm}$-Kr work described above, and the $e^{\pm}$-He, Ne, and Ar work described in Ref. 1). The existence of the shoulder in the e^--Xe curve near 20 eV raises the possibility that there could be a significant contribution to the total cross section from an inelastic process (or processes) in that vicinity, unless the elastic cross section possesses this intriguing shape. The e^--Xe ionization cross sections measured by Rapp and Englander-Golden[23] (which gradually increase from the ionization threshold of 12.13 eV, reaching a maximum value near 120 eV) would not explain the existence of a shoulder near 20 eV in the total-cross-section curve. Excitation cross sections for e^--Xe have been measured by Schiavone *et al.*[24] to the higher Rydberg states ($n=20-80$) and by Zapesochnyi and Feltsan[25] to the Paschen $2p_8$ levels. The shapes of the excitation cross-section curves obtained by these groups are consistent with what we would expect to be required to explain the shoulder in that they rise rapidly reaching a maximum at 20 eV or less, after which they decrease rapidly by a factor of 2 or more before reaching 40 eV, and finally change to a slowly decreasing function of energy. Although the magnitudes of these particular measured excitation cross sections are much too small to account for the observed shoulder, it may be that, when all possible excitations are considered, one could explain the observed shoulder.[26] The broad, flat nature of the peak in the present e^+-Xe curve also suggests the possibility of a significant contribution to Q_T in that vicinity (10—25 eV) from inelastic processes besides Ps formation. Above about 90 eV, the e^--Xe results remain higher than the e^+-Xe results up to the highest energies studied.

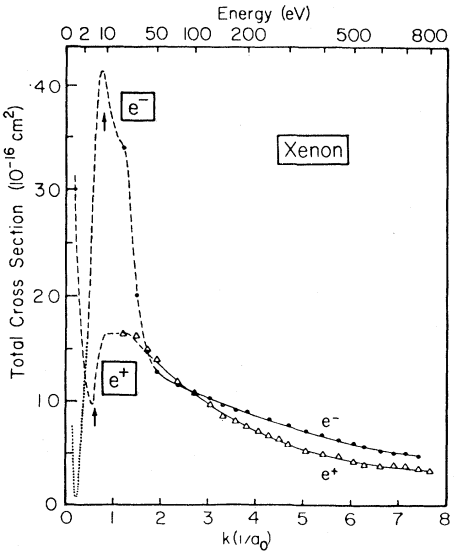

FIG. 7. A comparison of total $e^{\pm}$-Xe cross-section measurements. The present intermediate-energy measurements are indicated by the symbols. The solid curves are drawn through the present intermediate-energy measurements above the range of the earlier low-energy measurements of Dababneh *et al.* (Ref. 6), which are represented by dashed curves. The low-energy electron measurements of Ramsauer (Ref. 17) are represented by the dotted curve. The lowest-energy inelastic thresholds for each projectile are indicated by arrows and correspond to positronium formation at 5.33 eV for positrons and atomic excitation at 8.31 eV for electrons.

Note added in proof. A recent article by L. T. Sin Fai Lam [J. Phys. B 15, 119 (1982)] has made us aware of the existence of a shoulder in calculations of the e^--Xe elastic cross section in the vicinity of 20 eV, which could be responsible for a significant portion of the observed shoulder in our measured total cross sections.

ACKNOWLEDGMENTS

We gratefully acknowledge the helpful assistance of S. Smith and P. Felcyn in various aspects of this project. This work was supported by the National Science Foundation under Grant Nos. PHY77-18760 and PHY80-07984.

APPENDIX

In Table III we present our $e^{\pm}$-Kr and Xe intermediate-energy total-cross-section results.

TABLE III. Present total-cross-section results (in units of 10^{-16} cm^2) for intermediate-energy positrons and electrons colliding with Kr and Xe. The statistical uncertainties are enclosed in parentheses.

Energy (eV)	e^+-Kr	e^--Kr	e^+-Xe	e^--Xe
20	10.44(0.16)	23.10(0.04)	16.60(0.13)	34.06(0.04)
30	10.94(0.18)	18.60(0.03)	16.40(0.30)	20.20(0.04)
40	10.60(0.13)	16.05(0.04)	14.90(0.20)	14.86(0.03)
50	9.80(0.10)	14.45(0.03)	14.10(0.20)	12.95(0.02)
75	9.12(0.12)	11.84(0.02)	11.95(0.15)	11.65(0.02)
100	8.35(0.10)	10.44(0.02)	10.85(0.10)	10.83(0.02)
125	7.70(0.11)	9.36(0.02)	9.83(0.12)	10.42(0.02)
150	7.00(0.10)	8.55(0.02)	8.70(0.10)	9.78(0.02)
175	6.50(0.11)	7.75(0.02)	8.30(0.15)	9.29(0.01)
200	6.15(0.11)	7.39(0.02)	7.70(0.10)	9.10(0.02)
225			7.30(0.15)	
250	5.55(0.14)	6.54(0.02)	6.80(0.10)	8.41(0.02)
275			6.50(0.15)	
300	5.10(0.10)	5.97(0.02)	6.00(0.10)	7.87(0.01)
350	4.50(0.10)	5.54(0.01)	5.33(0.10)	7.30(0.01)
400	4.10(0.20)	5.07(0.01)	5.06(0.12)	6.92(0.01)
450	3.90(0.10)	4.75(0.01)	4.90(0.10)	6.42(0.02)
500	3.58(0.10)	4.47(0.01)	4.30(0.10)	6.14(0.01)
550	3.50(0.10)	4.19(0.01)	4.00(0.10)	5.80(0.01)
600	3.20(0.10)	4.01(0.01)	3.85(0.10)	5.39(0.01)
650	3.10(0.10)	3.78(0.01)	4.00(0.10)	5.15(0.01)
700	3.00(0.10)	3.62(0.01)	3.87(0.10)	5.17(0.01)
750	2.90(0.10)	3.52(0.01)	3.66(0.10)	4.87(0.01)
800	2.60(0.10)		3.40(0.10)	

*Present address: Department of Physics, Yarmouk University, Irbid, Jordan.

†Present address: Bell Laboratories, Allentown, Pennsylvania 18103.

[1]W. E. Kauppila, T. S. Stein, J. H. Smart, M. S. Dababneh, Y. K. Ho, J. P. Downing, and V. Pol, Phys. Rev. A 24, 725 (1981).

[2]D. P. Dewangen and H. R. J. Walters, J. Phys. B 10, 637 (1977).

[3]W. E. Kauppila, T. S. Stein, and G. Jesion, Phys. Rev. Lett. 36, 580 (1976).

[4]W. E. Kauppila, T. S. Stein, G. Jesion, M. S. Dababneh, and V. Pol, Rev. Sci. Instrum. 48, 822 (1977).

[5]T. S. Stein, W. E. Kauppila, V. Pol, J. H. Smart, and G. Jesion, Phys. Rev. A 17, 1600 (1978).

[6]M. S. Dababneh, W. E. Kauppila, J. P. Downing, F. Laperriere, V. Pol, J. H. Smart, and T. S. Stein, Phys. Rev. A 22, 1872 (1980).

[7]T. S. Stein, W. E. Kauppila, and L. O. Roellig, Phys. Lett. 51A, 327 (1975).

[8]K. F. Canter, P. G. Coleman, T. C. Griffith, and G. R. Heyland, J. Phys. B 6, L201 (1973).

[9]P. G. Coleman, T. C. Griffith, G. R. Heyland, and T. R. Twomey, Appl. Phys. 11, 321 (1976).

[10]B. Jaduszliwer, A. Nakashima, and D. A. L. Paul, Can. J. Phys. 53, 962 (1975).

[11]J-S. Tsai, L. Lebow, and D. A. L. Paul, Can. J. Phys. 54, 1741 (1976).

[12]A. G. Brenton, J. Dutton, F. M. Harris, R. A. Jones, and D. M. Lewis, J. Phys. B 10, 2699 (1977).

[13]A. G. Brenton, J. Dutton, and F. M. Harris, J. Phys. B 11, L15 (1978).

[14]T. C. Griffith, G. R. Heyland, K. S. Lines, and T. R. Twomey, Appl. Phys. 19, 431 (1979).

[15]R. P. McEachran, A. D. Stauffer, and L. E. M. Campbell, J. Phys. B 13, 1281 (1980).

[16]T. F. O'Malley, L. Spruch, and L. Rosenberg, J. Math. Phys. 2, 491 (1961).

[17]C. Ramsauer, Ann. Phys. (Leipzig) 72, 345 (1923); C. Ramsauer and R. Kollath, Ann. Phys. (Leipzig) 3, 536 (1929).

[18]F. J. de Heer, R. H. J. Jansen, and W. van der Kaay,

J. Phys. B 12, 979 (1979).
[19]R. W. Wagenaar and F. J. de Heer, J. Phys. B 13, 3855 (1980).
[20]I. E. McCarthy, C. J. Noble, B. A. Phillips, and A. D. Turnbull, Phys. Rev. A 15, 2173 (1977).
[21]K. F. Canter, P. G. Coleman, T. C. Griffith, and G. R. Heyland, Appl. Phys. 3, 249 (1974).
[22]P. G. Coleman, J. D. McNutt, L. M. Diana, and J. T. Hutton, Phys. Rev. A 22, 2290 (1980).
[23]D. Rapp and P. Englander-Golden, J. Chem. Phys. 43, 1464 (1965).
[24]J. A. Schiavone, S. M. Tarr, and R. S. Freund, Phys. Rev. A 20, 71 (1979).
[25]I. P. Zapesochnyi and P. V. Feltsan, Opt. Spectrosc. 20, 291 (1966).